THE JOURNAL OF PHYSICAL CHEMISTRY B

ARTICLE

pubs.acs.org/JPCB

Structure of the Pyridine−Chloranil Complex in Solution: A Surprise from Depolarized Hyper-Rayleigh Scattering Measurements

Ravindra Pandey,[†] S. Mukhopadhyay,[‡] S. Ramasesha,[‡] and Puspendu K. Das*[,†]

[†]Department of Inorganic and Physical Chemistry, Indian Institute of Science, Bangalore 560012, India

[‡]Solid State and Structural Chemistry Unit, Indian Institute of Science, Bangalore 560012, India

ABSTRACT: In this article, we report the structure of a 1:1 charge transfer complex between pyridine (PYR) and chloranil (CHL) in solution ($CHCl_3$) from the measurement of hyperpolarizability (β_{HRS}) and linear and circular depolarization ratios, D and D', respectively, by the hyper-Rayleigh scattering technique and state-of-the-art quantum chemical calculations. Using linearly (electric field vector along X) and circularly polarized incident light, respectively, we have measured two macroscopic depolarization ratios $D = I_{X,X}^{2\omega}/I_{X,Z}^{2\omega}$ and $D' = I_{X,C}^{2\omega}/I_{Z,C}^{2\omega}$ in the laboratory fixed XYZ frame by detecting the second harmonic (SH) scattered light in a polarization resolved fashion. The stabilization energy and the optical gap calculated through the MP2/cc-pVDZ method using Gaussian09 were not significantly different to distinguish between the cofacial and T-shape structures. Only when the experimentally obtained β_{HRS} and the depolarization ratios, D and D', were matched with the theoretically computed values from single and double configuration interaction (SDCI) calculations performed using the ZINDO-SCRF technique, we concluded that the room temperature equilibrium structure of the complex is cofacial. This is in sharp contrast to an earlier theoretical prediction of the T-shape structure of the complex.

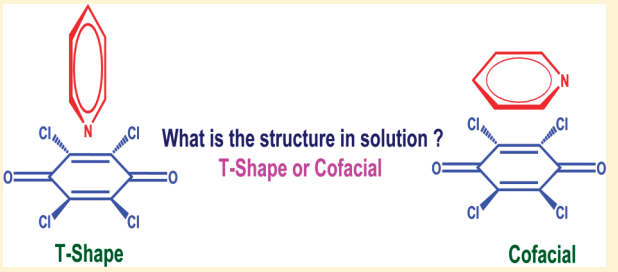

INTRODUCTION

Charge transfer (CT) complexes between small organic systems have always evoked great interest because at the molecular level, they provide the basis for understanding the stability and structure of large complex assemblies in chemistry and biology.[1−4] Some of these complexes have been investigated by NMR spectroscopy for determining their structures in solution, but certain intricate details have been missing from the structures/geometries that were proposed from NMR data. For example, Sung et al.[5] have measured the association constants of 1:1 charge transfer molecular complexes between 1,3,5-trinitrobenzene (TNB) and various substituted indoles using the relative chemical shifts of the protons of substituted indoles by NMR spectroscopy. They obtained different association constants for the same CT complex when the relative chemical shifts of different protons on the indoles were used. They could not provide any concrete evidence about the structure of the complex from their studies. Years later, Laatikainen et al.[6] studied the aromatic−aromatic interactions of benzene and hexafluorobenzene using proton−proton dipolar coupling in a strong magnetic field. From the magnitude of the proton−proton coupling constants, they guessed that there is a T-shape structure contribution in the benzene dimer, in the 1:1 benzene−naphthalene complex, etc., but the benzene−hexafluorobenzene dimer favors a structure that is parallel-stacked. Only a qualitative idea about the structure/geometry was discerned from the single dipolar coupling constant parameter measured experimentally. Recently, we have shown that polarization resolved hyper-Rayleigh scattering measurements, which give three experimental quantities to fit a structure along with quantum chemical calculations, provide more quantitative information about the structure/geometry of such complexes in solution.[7,8]

Formation of a weak CT complex between chloranil and pyridine derivatives in solution has been reported earlier by various spectroscopic and thermochemical methods,[9−11] but those studies were not directed toward structure/geometry elucidation of the complex. Some idea about the geometry of the pyridine−chloranil 1:1 complex came recently from a theoretical calculation by Li et al.[12] where they have shown that pyridine binds to chloranil via an effective $\sigma-\pi$ type interaction to form an inclined T-shape structure, with the pyridine plane making an angle of 77.8° to the chloranil plane in which the nitrogen atom of pyridine is pointed toward the center of the chloranil molecule. This is an interesting prediction since the proposed structure is close to the T-shape structure, which is rare in occurrence among organic aromatic molecular complexes. However, this calculated structure has not been probed experimentally. In this article, we have chosen a 1:1 molecular complex of pyridine (PYR) and chloranil (CHL) and investigated its structure/geometry by using the polarization resolved HRS method. It is important to realize that the 1:1 CT complexes exist in different isomeric orientational conformers in solution.

Received: September 15, 2011
Revised: October 25, 2011
Published: October 26, 2011

dx.doi.org/10.1021/jp2088934 | J. Phys. Chem. B 2011, 115, 13842–13846

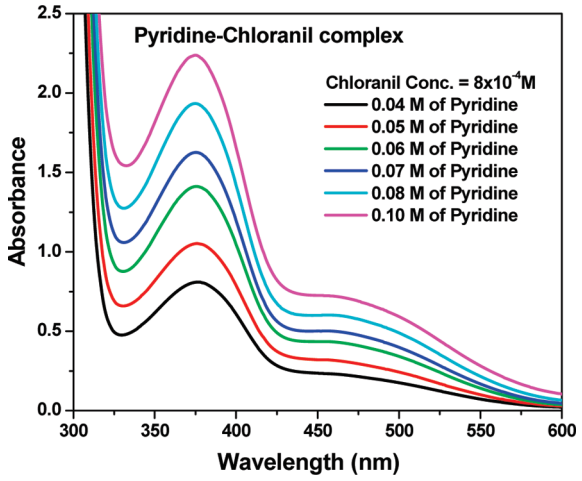

Figure 1. UV−visible spectra of the PYR−CHL 1:1 complex with different pyridine concentrations.

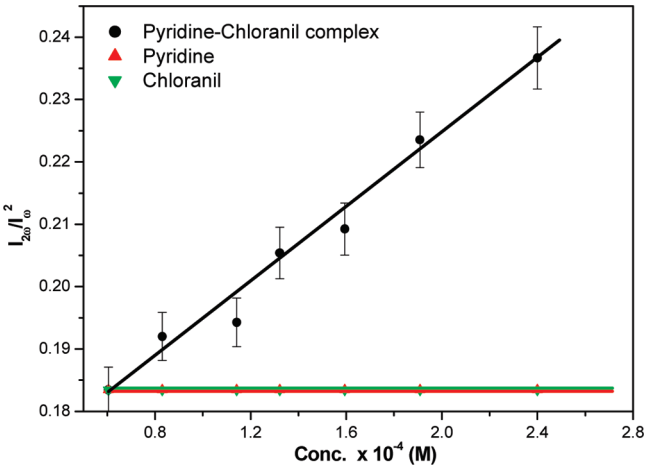

Figure 2. Normalized second harmonic intensity, $I_{2\omega}/I_{\omega}^{2}$, as a function of concentration of the PYR−CHL complex.

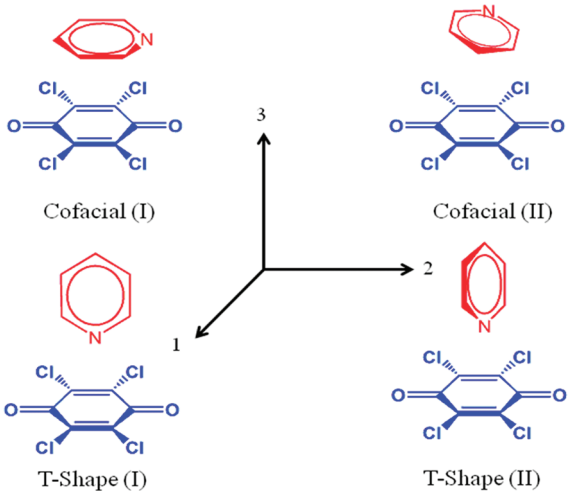

Figure 3. Four different conformations of the PYR−CHL complex. For all of the conformations, the center of the coordinate axis is placed in the middle of the CHL molecule, and the PYR moiety is displaced along the 3-axis.

The stabilization energy of these isomers differs by a very small amount of energy (typically of the order of a few kcal/mol). Thus, it is possible that at room temperature in solution a distribution of multiple conformations is present and the conformers collectively contribute to the measured hyperpolarizability. However, it is also possible that one or two conformers having significantly higher binding energy have a dominant contribution to the measured hyperpolarizability. Therefore, in order to determine the geometry of these complexes in solution, it is important to explore the structure−property relationship in a large number of different geometries of the PYR−CHL complex. To address this, quantum chemical calculations were performed to compute the linear and nonlinear optical properties in different conformations of the PYR−CHL complex. By comparing the calculated properties with experimental values, we infer about the predominant structure of the complex in solution.

EXPERIMENTAL SECTION

PYR and CHL of 99% purity were obtained from Sigma-Aldrich. The solvent used in the experiments was chloroform of HPLC grade (SD Fine Chemicals).

UV−Vis Spectroscopy. The UV−visible spectra of the PYR−CHL complex were recorded in a Perkin-Elmer (Λ-35) double beam spectrometer. For the measurement of β_{HRS} of the complex, the value for the concentration of the complex in solution is necessary, which was obtained from its molar extinction coefficient. The molar extinction coefficient was quantitatively estimated using the Benesi−Hildebrand method by titrating PYR against CHL.[13] A fixed concentration of CHL ($\sim 8 \times 10^{-4}$ M) was mixed with different concentrations of PYR (0.04−0.10 M). The mixtures were left for 2 h to equilibrate. The formation of the CT complex was marked by the appearance of the CT band at 466 nm. For the formation of the 1:1 complex exclusively, the PYR concentration was kept at least 50 times greater than that of CHL.

The concentration of the complex in solution was obtained from the value of the molar extinction coefficient, which was 3731 M^{-1} cm^{-1}. The association constant for the complex was calculated to be 2.0 M^{-1}. The UV−visible spectra of the PYR−CHL complex in $CHCl_3$ are shown in Figure 1. Mukherjee et al.[7] have suggested that the visible band at 466 nm is due to a $n-\pi^*$ transition: an electron from the lone pair on the pyridine-nitrogen atom goes to the empty π^* orbital of chloranil. The band at 374 nm corresponds to a $\pi-\pi^*$ transition where an electron from the occupied π orbital of pyridine is excited to the empty π^* orbital of chloranil. The visible band at 466 nm has been used for the determination of the molar extinction coefficient of the complex. The 374 nm band was not used since CHL also absorbs at the same wavelength.

Polarization Resolved HRS Measurements. The details of the unpolarized and polarization resolved HRS technique have been described in detail earlier.[14,15] The measurement was carried out at 1064 nm using the fundamental of a Q-switched Nd:YAG laser. The energy of the laser beam was kept as low as possible (<15 mJ/pulse) so that the dielectric breakdown or other nonlinear optical processes like self-induced (de)focusing, Brillouin scattering, etc. were avoided. The incident beam was focused by a plano-convex lens (focal length = 20 cm) to a point 2−3 cm ahead of the center of the cell. The incoherently scattered SH photons were collected at 90° using a set of

dx.doi.org/10.1021/jp2088934 |J. Phys. Chem. B 2011, 115, 13842–13846

collection optics and were made to fall on a visible PMT. The output from the PMT was digitized and averaged over 512 shots on a 500 MHz digital storage oscilloscope. For the measurement of β of the PYR−CHL complex, the external reference method was used and *para*-nitroaniline (PNA) was used as the reference. The quadratic power dependence of HRS intensities on incident laser power was checked prior to β measurements. In polarization resolved HRS experiments, the fundamental light beam polarized in the *X*-direction was allowed to propagate in the *Z*-direction, and the SH scattered light was collected in the *Y*-direction. A high power calcite Glan laser polarizer with a broadband antireflection coating was used at 1064 nm. A polarcor polaroid sheet was used as an analyzer to choose the two states of polarization of the SH light.

In this experimental configuration, the macroscopic linear depolarization ratio D in the laboratory fixed frame (XYZ) is then defined as[16−18]

$$D = \frac{I^{2\omega}_{X,X}}{I^{2\omega}_{Z,X}} = \frac{\langle {\beta_{XXX}}^2 \rangle}{\langle {\beta_{ZXX}}^2 \rangle} \quad (1)$$

During the standardization of the polarization setup, D for pNA in chloroform was measured and it was found to be 4.92, which matched the literature.[19,20] A quarter waveplate was placed after the polarizer to produce the circularly polarized light. The macroscopic depolarization ratio for the circularly polarized light is given by

$$D' = \frac{I^{2\omega}_{X,C}}{I^{2\omega}_{Z,C}} = \frac{\langle {\beta_{XYY}}^2 \rangle + \langle {\beta_{XXX}}^2 \rangle + \langle (\beta_{YXX} + \beta_{XXY})^2 - 2\beta_{XYY}\beta_{XXX} \rangle}{\langle {\beta_{ZYY}}^2 \rangle + \langle {\beta_{ZXX}}^2 \rangle + \langle (\beta_{ZYX} + \beta_{ZXY})^2 - 2\beta_{ZYY}\beta_{ZXX} \rangle} \quad (2)$$

D' of pNA was determined, and it was found to be 2.98, which matches the reported value.[19] For an unpolarized SH scattered light detection, as is done in normal HRS experiments, both β_{XXX} and β_{ZXX} contribute to the total signal intensity related to $\langle {\beta^2}_{HRS} \rangle$, which is given by

$$\langle {\beta_{HRS}}^2 \rangle = \langle {\beta_{XXX}}^2 \rangle + \langle {\beta_{ZXX}}^2 \rangle \quad (3)$$

The magnitude of β_{HRS}, D, and D' values depend on the tensorial components of β that appear in eqs 1−3, which in turn, are strongly dependent on the structure in which the two molecules are held together in the complex and the direction of dipole moments in the complex. These tensorial components change with a change in the relative orientation of the two molecules forming the complex. In other words, information about the structure of the complex can be derived from the values of β_{HRS}, D, and D' via the computational path.

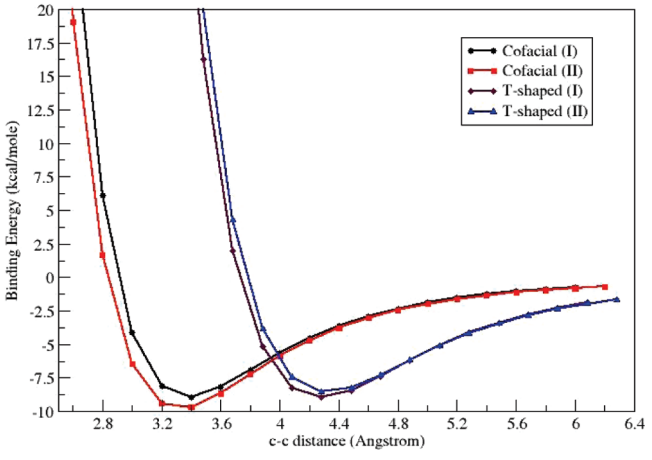

Figure 4. Variation of binding energies with the increase in the distance between the PYR and CHL molecule along the 3-axis for cofacial and T-shape conformations in the gas phase. The energies of all of the conformations are obtained at the MP2/6-31g** level without using the CP correction.

RESULTS AND DISCUSSION

The plot of normalized second harmonic intensity, $I_{2\omega}/{I_\omega}^2$, as a function of the concentration of the PYR−CHL complex as determined from its molar extinction coefficient is shown in Figure 2.

The β_{HRS} of the reference, pNA, is 7.2×10^{-30} esu in $CHCl_3$ at 1064 nm, and this value is used for the calculation of β_{HRS} for the PYR−CHL complex, which is found to be 25.7×10^{-30} esu. The measured β_{HRS} for pyridine and chloranil are 0.21×10^{-30} esu and 5.2×10^{-30} esu, respectively. The hyperpolarizabilities of both of these molecules are very small compared to that of the complex. This indicates that the enhancement of β_{HRS} is due to the charge transfer from PYR to the CHL. In addition, the measured macroscopic depolarization ratios, D and D' of the complex are found to be 4.94 and 2.99, respectively. These values of D and D' indicate that the complex is close to C_{2v} symmetry. Thus, the structure could either be T-shaped or cofacial. If we assign the structure of the PYR−CHL complex as T-shape, as assigned from Li's calculation,[12] we will be in serious disagreement with the nonlinear optical properties, β_{HRS}, D, and D' as computed using Zerner's intermediate neglect of differential overlap correction vector (ZINDO-CV) programs.[21] In order to compute linear and nonlinear optical properties, the geometry of the pyridine−chloranil

Table 1. Structural Parameters Such As the Angle between the PYR and CHL Planes, Center−Center (c−c) Distances, and Binding Energies of the Different Conformers of the PYR−CHL Complex[a]

phase	dimer conformations	angle (deg)	c−c distance (Å)	binding energy (kcal/mol)
gas phase	cofacial	8.9	3.45	−6.57
	cofacial-twisted	4.2	3.41	−6.38
	T-shape	90.0	4.40	−6.56
solution phase (chloroform)	cofacial	8.7	3.25	−10.83
	cofacial-twisted	9.2	3.25	−10.83
	T-shape	64.5	3.96	−9.67

[a] Both gas phase and solution phase data are presented.

(PYR−CHL) complex was optimized in the gas-phase and in a solvent dielectric (chloroform). It is important to choose the initial geometry carefully for geometry optimization. This is because there is a significant probability of getting trapped in a local minimum of slightly higher energy than the global ground state minimum. For this purpose, the PYR molecule was placed on top of the CHL moiety in four different orientations as depicted in Figure 3. While placing the two molecules close to one another, care was taken to avoid van der Waals contact between them. Starting from these four conformations, the distance between the two moieties along the 3-axis was increased in steps of 0.2 Å. The energies of all the conformations were calculated using the MP2/6-31g** method. The variation of binding energies with the distance between the two moieties is presented in Figure 4.

The energies of the cofacial structures were the lowest when the two moieties were separated by 3.2 Å (center-to-center distance), whereas the energies were the lowest for the T-shape structures at 4.1 Å. The energies for the cofacial conformations are 9.52 and 8.38 kcal/mol, whereas those of the T-shape structures are 9.19 and 8.97 kcal/mol. This implies that the T-shape structure is unstable by about 0.3 kcal/mol with respect to the cofacial structure. This is in contradiction to what was predicted by the DFT calculations of Li et al.[8] where a bound cofacial structure is not found, and thus, the T-shape structure was assigned as the ground state structure. In order to resolve this issue theoretically, we decided to use cc-pVDZ basis sets, which accounts for better incorporation of the correlation energy.[22] In addition, we have taken care of the basis-set superposition error (BSSE) using the counterpoise (CP) correction method. To include solvent effects, geometry optimizations were performed using the polarizable continuum model (PCM) as implemented in Gaussian09. All geometry optimizations were followed by vibrational frequency calculations in order to make sure that the true ground state potential energy surface (PES) was obtained. The binding energies and some of the structural parameters are listed in Table 1. The gas-phase optimized structures are presented in Figure 5.

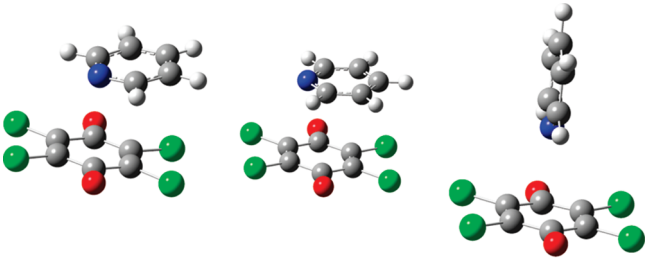

Figure 5. Gas-phase optimized conformations of the PYR−CHL complex: (i) cofacial, (ii) cofacial-twisted, and (iii) T-shape conformations. The chlorine atoms are marked in green, the oxygen atoms are marked in red, the nitrogen atom is marked in blue, the carbon atoms are marked in gray, and the hydrogen atoms are marked in white.

Starting from the two different cofacial structures, the optimization procedure leads to two different structures of similar binding energy, whereas both the T-shape conformations lead to one low energy structure (Table 1). In solution, all the conformations have higher binding energies compared to those of their gas phase counterparts. This is due to stabilization of the CT complex in the solvated state accompanied by the lowering of the c−c distances. In the gas phase, there is hardly any difference between the stabilization energies of the cofacial and T-shape structures; however, the presence of chloroform makes the cofacial isomer more stable. Li et al.[8] could not observe the bound cofacial structure because frequently used DFT functionals such as PBE used by Li et al. are not sufficient for predicting the ground state structure correctly in these weakly bonded complexes. This is also one of the main motivations for developing the range-separated ω-functionals.[23,24]

The calculations of linear and nonlinear optical properties of the PYR−CHL complex in various conformations were then performed using the ZINDO-CV-SCRF programs. The ground and the excited state properties were obtained using the single and double configuration interactions (SDCI) method, which is augmented with the SCRF model in order to incorporate the solvent effects. The active space for the single particle-hole excitations includes 35 highest occupied levels and 28 lowest unoccupied levels, whereas that for the double particle-hole excitations incorporates 4 highest occupied levels and 4 lowest unoccupied levels. This method was previously used to calculate the ground and excited state electronic properties for different CT complexes.[8] Using the eigen-values and eigen-states obtained from CI calculations, we calculated the hyperpolarizibility (β) tensor components, which were subsequently used to compute the β_{HRS} and the linear and circular depolarization ratios as described earlier. Table 2 lists the NLO properties of the PYR−CHL complex in chloroform.

For the cofacial and the cofacial-twisted complex, the $n-\pi^*$ (~2.85 eV) and the $\pi-\pi^*$ (~3.26 eV) transitions match well with the experimental absorption peaks of the complex at 2.66 and 3.31 eV, respectively. The optically forbidden first excited state is mainly dominated by the HOMO − 6 → LUMO + 3

Table 2. Theoretical Excitation Energies, Oscillator Strengths (o.s.), β_{HRS}, and Linear and Circular Depolarization Ratios (D and D') of Different Structures of the PYR−CHL Complex in Chloroform[a]

structure of the complex	optical gap (eV) (o.s.)	β_{HRS} (esu × 10^{-30})	D	D'
cofacial (theory)	2.84 (0.00)	20.16	4.63	2.72
	3.25 (0.10)			
cofacial-twisted (theory)	2.85 (0.00)	19.92	4.62	2.71
	3.26 (0.10)			
T-shape (theory)	2.77 (0.00)	4.62	2.34	1.80
	4.00 (0.20)			
exptl	2.66 (0.04)[b]	25.7	4.94	2.99
	3.31 (0.19)			

[a] Experimental data is shown in the last row for comparison. [b] Experimental oscillator strengths were obtained from the two observed absorption bands of the complex using standard procedures.

dx.doi.org/10.1021/jp2088934 |J. Phys. Chem. B 2011, 115, 13842–13846

excitation. In this transition, the charge on the lone pair in (HOMO − 6) is transferred to (LUMO + 3) in which the charge lies in the π^* orbital and is thus characterized as the $n \rightarrow \pi^*$ transition. However, the second transition is dominated by the HOMO → LUMO transition which is centered on the carbon and nitrogen p_z orbitals of the PYR and CHL moieties and can be characterized as the $\pi \rightarrow \pi^*$ transition. Both of the excited states are associated with the CT from the PYR to CHL. For the T-shape conformer, the $n-\pi^*$ transition is off by only 0.11 eV from the experimental value, but the $\pi-\pi^*$ transition is overestimated by ∼0.7 eV. We compute the NLO coefficients of the PYR−CHL complex for all the three different conformations. The cofacial conformers exhibit significantly larger β_{HRS} compared to that of the T-shape conformer. This is perhaps due to the stronger $\pi-\pi$ interaction between the PYR and CHL molecules in the cofacial conformation than in the T-shape structure, which facilitates the charge transfer from the PYR to the CHL moiety. The experimental β_{HRS}, the linear and circular depolarization ratios compare well with those of the cofacial structures. For the T-shape structure, the computed β_{HRS}, D, and D' values are all significantly lower than the experimental values. Therefore, by comparing the measured NLO properties with computed values, we rule out the possibility of the T-shape structure for the PYR−CHL complex in solution at room temperature. We also found that the orientation of the pyridine molecule with respect to the chloranil molecule as shown in the cofacial twisted structure does not alter the linear and nonlinear optical properties significantly, and thus, we infer that the complex has a cofacial structure in solution.

CONCLUSIONS

In this article, we have reported the equilibrium ground state structure of the PYR−CHL complex in solution by depolarized HRS experiment and quantum chemical calculations. In fact, without computation of β-tensors for various structures, it was tempting to assign the structure as the T-shape from previous calculations reported in the literature, symmetry arguments, and experimental values of β_{HRS}, D, and D'. When the computed values of nonlinear optical properties (β_{HRS}, D, and D') were matched with experimental values, we found that the ground state structure of the complex in solution is cofacial, which is contrary to previous calculation done on the complex that predicted a T-shape structure. However, a cofacial structure is less unexpected intuitively from a good $\pi-\pi$ interaction point of view within a molecular orbital (MO) picture. The results drive home two important points regarding the structure−NLO property relationship in weakly bonded complexes: (1) while studying their stability, one needs to be cautious about the type of basis sets and quantum chemical methods to be adopted for reliable calculation; and (ii) more importantly, matching only the optical gaps of various conformations from calculation with experimental values may not necessarily lead to the correct assignment of the structure. One requires many experimental quantities (optical gap and three NLO properties in the present example) to match the theory for the correct prediction of the structure. This article also demonstrates the usefulness of the polarization resolved HRS method in structure elucidation in solution.

AUTHOR INFORMATION

Corresponding Author

*Fax: 91-80-2360 0683. E-mail: pkdas@ipc.iisc.ernet.in.

ACKNOWLEDGMENT

R.P. and S.M. thank the CSIR, Government of India, for Senior Research Fellowships. P.K.D. and S.R. are thankful to the DST, Government of India, for generous funding.

REFERENCES

(1) Meyer, E. A.; Castellano, R. K.; Diederich, F. *Angew. Chem, Int. Ed.* **2003**, *42*, 1210–1250.
(2) Waters, M. L. *Curr. Opin. Chem. Biol.* **2002**, *6*, 736–741.
(3) Černý, J.; Hobza, P. *Phys. Chem. Chem. Phys.* **2007**, *9*, 5291–5303.
(4) Mahalakshmi, R.; Raghothama, S.; Balaram, P. *J. Am. Chem. Soc.* **2006**, *128*, 1125–1138.
(5) Sung, M. T.; Parker, J. A. *Proc. Natl. Acad. Sci. U.S.A.* **1972**, *69*, 1196–1200.
(6) Laatikainen, R.; Ratilainen, J.; Sebastian, R.; Santa, H. *J. Am. Chem. Soc.* **1995**, *117*, 11006–11010.
(7) Pandey, R.; Ghosh, S.; Mukhopadhyay, S.; Ramasesha, S.; Das, P. K. *J. Chem. Phys.* **2011**, *134*, 044533:1–8.
(8) Mukhopadhyay, S.; Pandey, R.; Das, P. K.; Ramasesha, S. *J. Chem. Phys.* **2011**, *134*, 044534:1–8.
(9) Ray, A. K.; Bhattacharya, S.; Banerjee, M.; Mukherjee, A. K. *Spectrochim. Acta, Part A* **2002**, *58*, 1375–1378.
(10) Bhattacharya, S.; Banerjee, M.; Mukherjee, A. K. *Spectrochim. Acta, Part A* **2001**, *57*, 2409–2416.
(11) Mukherjee, D. C.; Chandra, A. K. *Spectrochim. Acta* **1963**, *19*, 731–739.
(12) Li, Z.-Y.; Wang, H.-L.; He, T.-J.; Liu, F.-C.; Chen, D.-M. *J. Mol. Struct.* **2006**, *778*, 69–76.
(13) Benesi, H. A.; Hildebrand, J. H. *J. Am. Chem. Soc.* **1949**, *71*, 2703–2707.
(14) Ghosh, S. Ph.D. Thesis, Indian Institute of Science, Bangalore, India, 2008.
(15) Ghosh, S.; Das, P. K. *Proc. SPIE* **2009**, *7413*, 74130N–9.
(16) Bershon, R.; Pao, Y. H.; Frisch, H. L. *J. Chem. Phys.* **1966**, *45*, 3184–3198.
(17) Zyss, J.; Ledoux, I. *Chem. Rev.* **1994**, *94*, 77–105.
(18) Cyvin, S. J.; Rauch, J. E.; Decius, J. C. *J. Chem. Phys.* **1965**, *43*, 4083–4095.
(19) Heesink, G. J. T.; Ruiter, A. G. T.; Hulst, N. F.; Bölger, B. *Phys. Rev. Lett.* **1993**, *71*, 999–1002.
(20) Kaatz, P.; Shelton, D. P. *J. Chem. Phys.* **1996**, *105*, 3918–3929.
(21) Ramasesha, S.; Shuai, Z.; Brédas, J.-L. *Chem. Phys. Lett.* **1995**, *245*, 224–229.
(22) Dunning, T. H. *J. Chem. Phys.* **1989**, *90*, 1007–1023.
(23) Chai, J.-D.; Head-Gordon, M. *J. Chem. Phys.* **2008**, *128*, 084106.
(24) Chai, J.-D.; Head-Gordon, M. *Phys. Chem. Chem. Phys.* **2008**, *10*, 6615–6620.